

CMS Internal Note

The content of this note is intended for CMS internal use and distribution only

June 19, 2002

COCOA Simulation of the EMU Alignment System

D. Eartly, R. Lee, K. Maeshima
Fermi National Accelerator Laboratory

Abstract

A general simulation of the CMS Endcap Muon Position Monitoring System (EMPMS) has been performed to evaluate the operational viability of the system as a whole, estimate the precision with which the system can reconstruct CSC chamber positions, and relate the contribution of uncertainties in the construction of individual components to the performance of the system as a whole. Simulations of an idealized EMU system were performed with COCOA v2.0.0. The simulations included all major system components and appropriate CSC chamber geometries. This report is a summary of the work presented in Ref [1].

1. COCOA Simulation of the Endcap Muon Alignment Scheme

A detailed description of the Endcap Muon Position Monitoring System (EMPMS) may be found in Reference [1] and [2]. The EMPMS system is charged with the determination and monitoring of Cathode Strip Chamber (CSC) locations and orientations in the Muon Endcap System. The system employs crosshair laser diodes and Digital CCD Optical Position Sensors (DCOPS) to determine CSC positions along three Straight Line Monitoring (SLM) laser lines and the positions of the iron Muon Endcap (ME) Layers upon which the all CSC chambers are mounted.

An object oriented model of an idealized EMPMS has been constructed in the framework of the CMS Object Oriented Code for Optical Alignment (COCO v2.0.0) [3]. COCOA allows the user to reconstruct the position and angles of optical objects in a given system as well as propagate associated (RMS) errors. The COCOA simulation includes all major system components and appropriate CSC chamber geometries. Since the system is idealized, it has been assumed that all measurement devices are able to make a successful measurement and the full redundancy of the alignment scheme (multiple measurements of opposing lasers) is exploited. The effects of component failure (missing CCD measurements from DCOPS, faulty laser modules, inadequate resolutions) should be examined separately.

2. Definition of Simulation Components and Uncertainties

All components of the EMPMS system have been included in the present COCOA simulation including CSC chambers, DCOPS sensors, inclinometers, and proximity sensors. The description and estimation of mechanical uncertainties on each component in the simulation is based upon official CMS production drawings. The operational performance of DCOPS and analog sensors in the simulation is taken from the findings of the full scale prototype of the partial system tested at the CERN ISR tunnel in the summer of 2000 [4].

The most important object in the simulation is the basic Cathode Strip Chamber (CSC) object. Of principle importance is the manner in which the chamber ‘center’ is related to the reference pin on the DCOPS sensors. Since tolerances between the separation of strip layers is not controlled in CSC chamber production, it has been decided to define a ‘Reference Center’ (or ‘Active Centerpoint’) for the chambers as the average strip position projected onto the upper strip plane. For a perfectly constructed CSC chamber (no uncertainties in construction), the geometrical centerline of the CSC chamber will fall along the Active Reference Center of the simulated chambers. The uncertainty between the Active Reference Center and primary DCOPS reference pin is estimated as $\pm 129 \mu\text{m}$ in the CMS $R\Phi$ plane and includes estimations of uncertainties arising from the distortion and shearing between CSC layers. Other uncertainties considered by the simulation include the LINK reconstruction of MAB positions ($\pm 135 \mu\text{m}$, $\pm 10 \mu\text{rad}$) and Secondary Link Lines on ME ± 1 ($\pm 10 \mu\text{m}$, $\pm 2 \mu\text{rad}$) [5] as well as uncertainties in the calibration of DCOPS sensors [6].

The final COCOA simulation script contained approximately 6200 separate objects to fit with at least 4700 non-zero correlations. A VRML model of the system constructed by COCOA is shown in Figure 1.

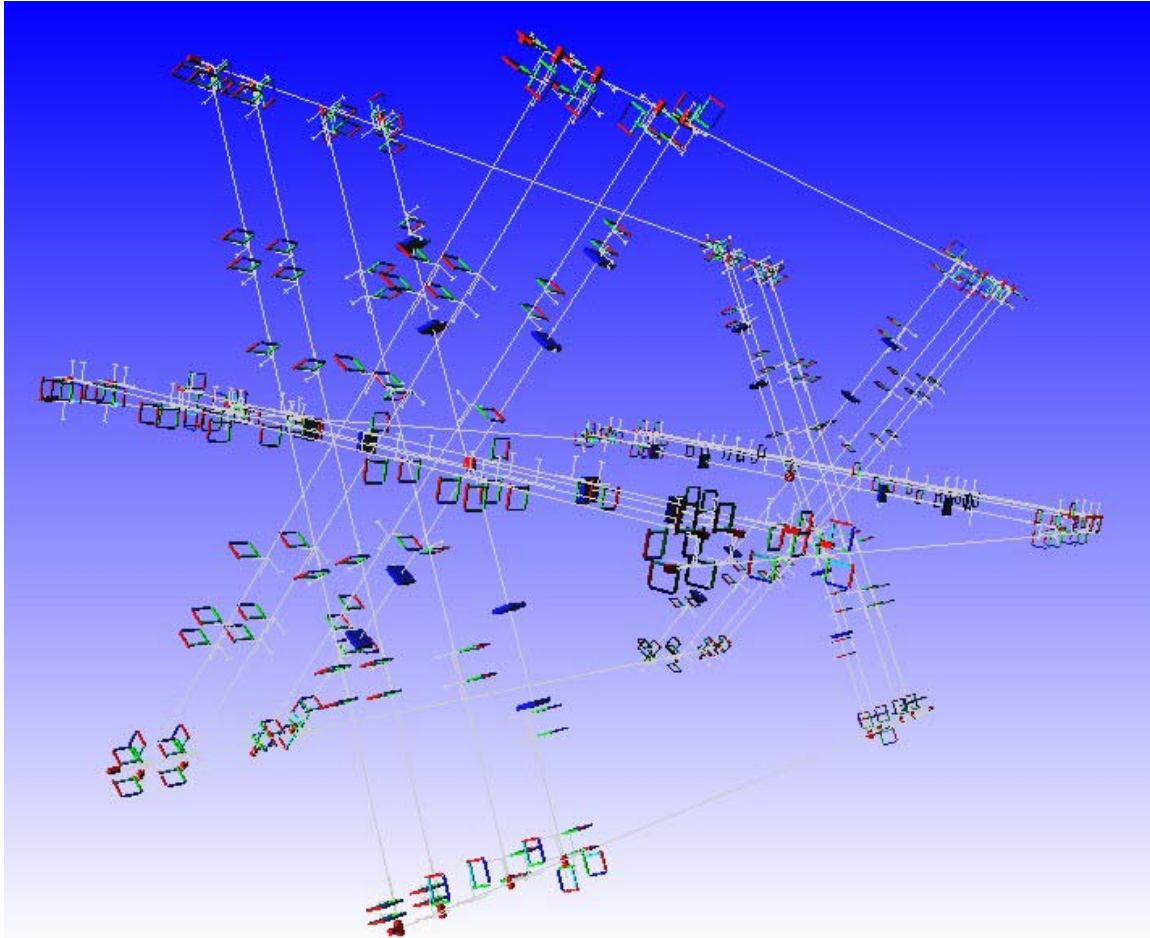


Figure 1: The Simulated EMU Alignment System. This is a COCOA generated VRML representation of the simulated geometry used for the idealized simulations of the EMU Alignment System.

3. Simulation Results

Using the full COCOA simulation model, several attempts were made to obtain a fit of the complete 8 ME disc system. These attempts failed with the computers reporting abnormal utilization and allocation of memory. Indeed, when the memory usage of the system was examined, it was found that the memory required for the storage of the resulting matrices exceeded the 1GB. The largest simulation successfully fit with the available memory was a complete ME ± 2 , ± 3 , ± 4 layer system (6 of 8 ME Layers + Transfer Laser Lines).

Fifty-three smaller subsets of the ME ± 2 , ± 3 , ± 4 Layers and Transfer Line simulation were also completed and compared amongst themselves and the larger 6 ME layer simulations. These subsets included all possible permutations of systems composed of at least two ME layers with full transfer line systems.

3.1. Comparison of Large Simulations vs. Small Simulations

Comparisons made between systems within the 53 subsets of two ME disc systems showed very little variation ($< 10\%$) between the certainties with which identical chambers could be reconstructed. Comparisons made between these two ME Layer systems and the larger six ME Layer system also yielded very little variation ($< 5\%$) between the uncertainties with which identical chambers could be reconstructed. This seems to confirm that there is very little coupling of components across different ME Layers.

3.2. Reconstruction of CSC Chambers Locations and Orientations

The uncertainty in spatial definition for CSC chambers along a particular SLM line may vary from the uncertainty of similar chambers in other SLM lines. However, the discrepancies between chamber uncertainties in ME Layers with the same SLM arrangement of components is expected to be small ($< 10\mu\text{m}$). For chambers in a given Endcap layer, these variations are primarily due to differences in the separation (i.e. lever arm) between transfer line and reference sensors located at the SLM endpoints. Likewise, variations in the size and type of CSC chambers across different ME Layers create similar discrepancies in the spatial definition of CSC chamber locations. Since SLM lines on ME ± 1 discs are constructed in a very different manner from those on SLM ME ± 2 , ± 3 , and ± 4 discs, more substantial variations are expected between chamber uncertainties when comparisons are made to ME ± 1 chambers. The mean uncertainty with which chamber locations and orientations along the SLM lines can be reconstructed in the EMU alignment scheme is summarized in Tables 2 and 3. The average deviations presented alongside the estimates represent the average deviation from the mean uncertainty for the all chambers of similar type or placement in the CMS detector.

The original ME ± 1 alignment scheme did not incorporate inclinometers on ME $\pm 1/2$ chambers. It had been assumed that the ME $\pm 1/3$ SLM lines, having been offset from the Secondary Link laser lines, would provide sufficient angular definition about the local chamber Z axis for the ME $\pm 1/2$ chambers (sensors on these chambers cannot discern rotations about the laser lines). Simulations of the ME ± 1 layer without inclinometers revealed poor spatial and rotational resolution on all ME ± 1 chambers. For this reason, inclinometers similar to those employed on the transfer plates were incorporated into the ME $\pm 1/2$ chamber frames. Simulations of the idealized system are performed with the resolution of these inclinometers set to be equivalent to the long term resolution of the inclinometers studied during the 2000 ISR tests.

CSC Chamber	Mean Uncertainty in Chamber Locations		Average Deviation of Uncertainty	
	CMS R Φ (μm)	CMS Z (μm)	CMS R Φ (μm)	CMS Z (μm)
ME \pm 1/2 (no inclinometer)	515	717	17	9
ME \pm 1/2 (σ inclinometer = short term ISR σ)	90	385	2	5
ME \pm 1/2 (σ inclinometer = long term ISR σ)	187	415	2	1
ME \pm 1/3	216	878	3	22
ME \pm 2/1	205	467	10	12
ME \pm 2/2	221	509	7	24
ME \pm 3/1	230	491	14	15
ME \pm 3/2	248	520	20	22
ME \pm 4/1	241	525	14	17
ME \pm 4/2	259	524	20	17

Figure 2: Uncertainty in CSC locations along the SLM lines for the Idealized EMU System. The uncertainty estimates for chambers in ME \pm 1/2 layer have been done using two sets of resolutions for the inclinometers placed on the ME \pm 1/2 CSC chamber frames.

CSC Chamber	Mean Uncertainty in Chamber Orientation		Average Deviation of Uncertainty	
	CMS R Φ (μrad)	CMS Z (μrad)	CMS R Φ (μrad)	CMS Z (μrad)
ME \pm 1/2 (inclinometer short term ISR σ)	95	95	N/A	N/A
ME \pm 1/2 (inclinometer long term ISR σ)	698	698	N/A	N/A
ME \pm 1/3	138	1168	3	360
ME \pm 2/1	113	812	0	252
ME \pm 2/2	74	771	0	297
ME \pm 3/1	834	888	244	261
ME \pm 3/2	742	777	303	323
ME \pm 4/1	725	909	383	241
ME \pm 4/2	1105	839	126	315

Figure 3: Uncertainty in CSC Orientations About Axes Parallel to CMS Coordinate System and Through CSC Chamber Centers in the Idealized EMU System. The uncertainty estimates for chambers in ME \pm 1/2 layer have been done using two sets of resolutions for the inclinometers placed on the ME \pm 1/2 CSC chamber frames.

3.3. Dependency of Reconstruction on DCOPS-Reference Center Uncertainties

Figure 4 shows how the uncertainties in the CMS RPhi position of the CSC chambers vary with the uncertainty in the chamber construction (along the chamber's local X axis). For all chambers, this relationship is linear. The slope indicates the correlation between uncertainties in chamber construction and reconstructed chamber RPhi positions is roughly 1:3, except on the ME $\pm 1/2$ chambers where it is closer to 1:4. The significantly higher correlation on the ME $\pm 1/2$ chambers is due to the much lower uncertainties associated with the definition of the Secondary Link lines and resolution of the ME $\pm 1/2$ LINK CMOS sensors. Correlations decrease slightly for chambers located in ME layers further away from the MABs as the net uncertainty is generally larger.

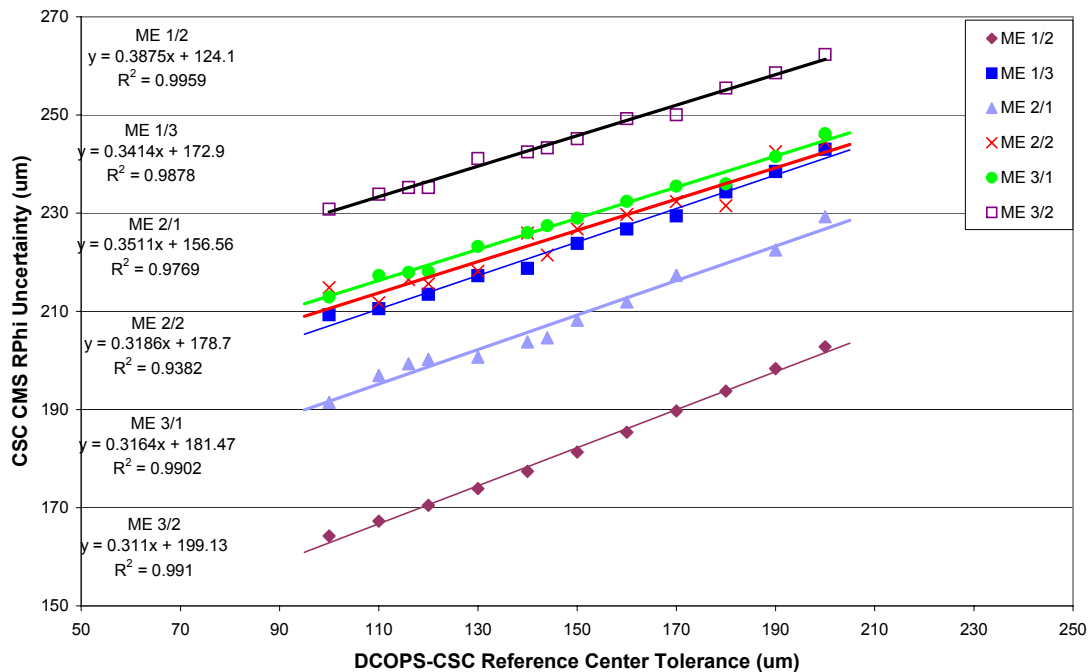


Figure 4: Reconstructed CSC RPhi Chamber Uncertainty vs. DCOPS-CSC Reference Center Tolerance. The plot shows the average uncertainty in reconstructed chamber locations as a function of the uncertainty estimate on the relative placement of the primary DCOPS calibration pin with the chamber reference centerpoint.

4. References

- [1] R. Lee. Simulation and Study of the CMS Endcap Alignment Scheme. PhD Thesis, Purdue University, 2002.
- [2] <http://home.fnal.gov/~maeshima/alignment/outline/outline.html>
- [3] Brunel, L., Simulation and Reconstruction Software for Opto-Geometrical Systems. CMS Note 1998/079, Nov 10, 1998.

P. Arce. CMS Object Oriented Code for Optical Alignment (COCOA). CMS NOTE-2002/001.
- [4] D. Eartly, R. Lee, K. Maeshima. ISR 2000 EMU Alignment Test Results Summary. CMS IN-2002/004.
- [5] Link Alignment Group, "Simulation and Performance", Muon Alignment EDR / Muon EDR-3 Documentation, Nov 2000.

Private communication with Pedro Arce, CERN, Nov 2000.
- [6] COPS Sensor Board Calibration, J. Moromisato et al, Oct 2000, unpublished.